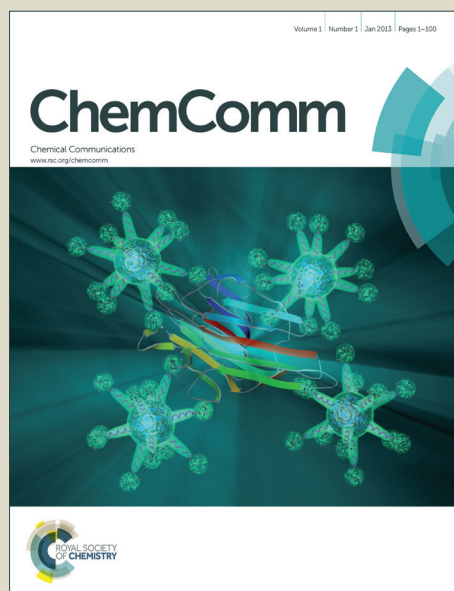


ChemComm

Accepted Manuscript



This is an *Accepted Manuscript*, which has been through the Royal Society of Chemistry peer review process and has been accepted for publication.

Accepted Manuscripts are published online shortly after acceptance, before technical editing, formatting and proof reading. Using this free service, authors can make their results available to the community, in citable form, before we publish the edited article. We will replace this *Accepted Manuscript* with the edited and formatted *Advance Article* as soon as it is available.

You can find more information about *Accepted Manuscripts* in the [Information for Authors](#).

Please note that technical editing may introduce minor changes to the text and/or graphics, which may alter content. The journal's standard [Terms & Conditions](#) and the [Ethical guidelines](#) still apply. In no event shall the Royal Society of Chemistry be held responsible for any errors or omissions in this *Accepted Manuscript* or any consequences arising from the use of any information it contains.

COMMUNICATION

Manipulation of Ionic Liquid Anion–Solute–Antisolvent Interactions for the Purification of Acetaminophen

Cite this: DOI: 10.1039/x0xx00000x

Received 00th January 2012,

Accepted 00th January 2012

DOI: 10.1039/x0xx00000x

www.rsc.org/chemcomm

Hydrogen bond donating cosolvents have been shown to significantly reduce the solubility of acetaminophen (AAP) in ionic liquids containing the acetate anion. Reduced solubility arises from competition for solvation by the acetate anion and can be used for the design of advanced separation techniques, illustrated by the crystallization of AAP.

Crystallization is one of the most industrially important methods of purification.¹ The solvent used for a crystallization process can influence the properties of the resultant solid with respect to crystal shape, polymorphism and impurity incorporation.² Solvent selection is limited by the competing demands whereby the initial solubility of the target is required alongside the ability to recover the target in significant yield with improved purity. In general, recovery of the target compound is accomplished through solvent evaporation, or changes in the temperature or solvent composition. The latter is typically performed by the addition of an antisolvent, conventionally a liquid within which the target exhibits poor solubility.

Ionic liquids (ILs), commonly defined as salts that melt below 100 °C,³ are a unique class of solvents that have attracted considerable research interest in recent years.⁴ ILs frequently exhibit low flammability,⁵ low vapor pressures,⁶ large liquidus ranges and good thermal stability as well as tunable physicochemical properties through the appropriate selection of cations and anions or the use of multiple ion combinations, i.e., IL mixtures or double salt ILs.⁷

ILs are being increasingly investigated for pharmaceutical applications as solvents for active pharmaceutical ingredients (APIs),⁸ their purification,⁹ and even as APIs themselves.¹⁰ Despite the interest in ILs as solvents for crystal engineering and the crystallization of nanomaterials,¹¹ few examples of ILs as solvents for the crystallization of APIs exist¹² and none, as far as the authors are aware, examine the use of ILs for the purification by crystallization of APIs. Our initial investigation in this area focuses on AAP as a model compound and the manipulation of intermolecular interactions to tailor its solubility using a novel antisolvent approach.

The presence of a strong hydrogen bond donating phenol moiety on AAP suggests that its solubility should be governed primarily by its interaction with the IL anion, as has been found for related compounds.¹³ If this were the case, then addition of a hydrogen bond donating cosolvent could disrupt these interactions and lead to the

potential for the design of not only the IL solvent but the antisolvent through consideration of the intermolecular interactions involved.

To investigate this hypothesis the solubility of AAP and its major impurity, 4-aminophenol (4-AP), which also possesses a phenolic group, was assessed in 5 different ILs at 25 °C (Table 1, structures and abbreviations in Fig. 1). The ILs chosen allowed hydrogen bonding effects on solubility to be isolated as they feature anions of different hydrogen bond basicity (increasing in the order bis(trifluoromethanesulfonyl)imide ([NTf₂]⁻) < [BF₄]⁻ < acetate ([OAc]⁻)) and cations of different hydrogen bond acidity (increasing in the order 1-butylpyridinium ([BPy]⁺) < 1-butyl-3-methylimidazolium ([BMIM]⁺) ≈ 1-ethyl-3-methylimidazolium ([EMIM]⁺) < 1-(2-hydroxyethyl)-3-methylimidazolium ([EtOHMIM]⁺).¹⁴

Table 1 Solubility data for the dissolution of AAP and 4-AP at 25 °C.

IL	AAP (mol%)	4-AP (mol%)
[EMIM][NTf ₂]	1.3	1.0
[BMIM][BF ₄]	9.7	6.6
[EMIM][OAc]	- ^a	- ^a
[BPy][BF ₄]	10.0	7.1
[EtOHMIM][BF ₄]	4.0	5.1

^a Solubility >40 wt%. Solution too viscous to stir before solubility limit was reached.

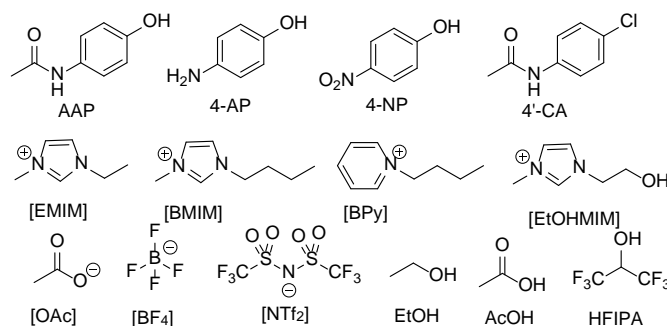


Fig. 1 Structures and abbreviations of compounds, solvents and ions.

As anticipated, the solubility of both AAP and 4-AP is governed primarily by basicity of the IL anion. This indicates that the

hydrogen bond acidity of the cation is of secondary importance as is clathrate

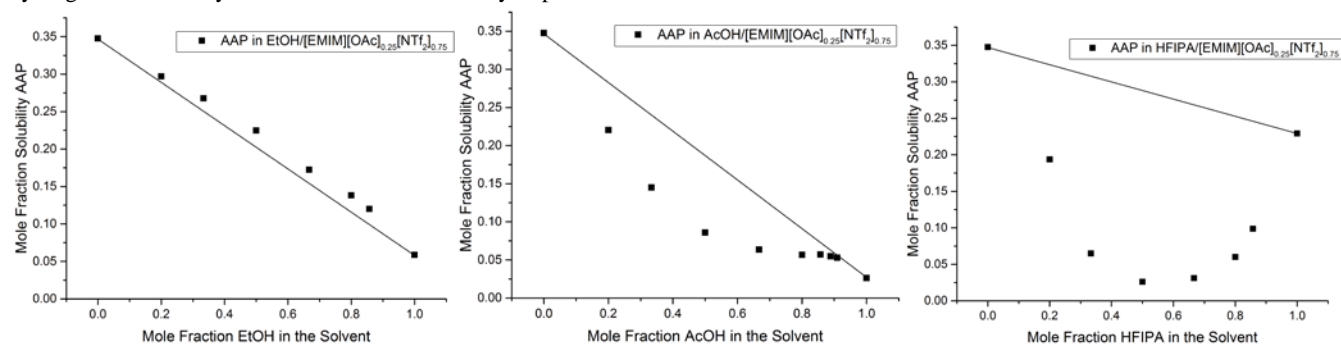


Fig. 3 Mole fraction solubility of AAP in mixed solvents of $[\text{EMIM}][\text{OAc}]_{0.25}[\text{NTf}_2]_{0.75}$ and (left to right) EtOH, AcOH and HFIPA.

formation around the aromatic solutes, which is generally favored by weaker cation–anion interactions.¹⁵ The more hydrogen bond acidic cations lead to reduced solubility, likely due to competition between the cation and the phenol group for solvation by the anion or reduced ion–quadrupole interactions due to stronger ion association.¹⁶

AAP has the highest solubility in $[\text{EMIM}][\text{OAc}]$ of the solvents tested. However, the high viscosity of $[\text{EMIM}][\text{OAc}]$ solutions with greater than 40 wt% solute precluded precise solubility measurement and would hinder crystallization processes conducted above such concentrations. For this reason, the use of ILs containing both $[\text{EMIM}][\text{OAc}]$ and the less viscous $[\text{EMIM}][\text{NTf}_2]$ were studied. Such mixtures have attracted interest recently due to their potential to more finely tune the physicochemical properties of the resultant ILs.⁷ Interestingly, the solubility of AAP and 4-AP in $[\text{EMIM}][\text{OAc}]_x[\text{NTf}_2]_{1-x}$ is linearly correlated with $[\text{OAc}]^-$ concentration (ESI). Moreover, the slopes of these lines are almost precisely 2, suggesting a specific 2:1 stoichiometric interaction between the phenols and $[\text{OAc}]^-$ ions. Similar strong hydrogen bonding interactions have been implicated in the formation of liquid versions of cocrystals and may account for this distinctive solubility behavior.¹⁷

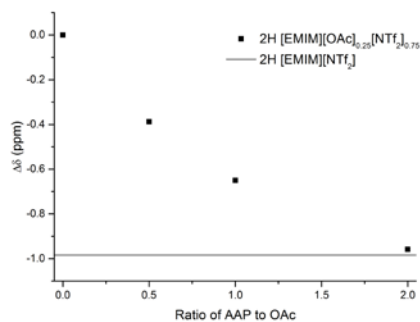


Fig. 2 ^1H NMR chemical shift of $[\text{EMIM}]^+$ 2-H resonance in $[\text{EMIM}][\text{OAc}]_{0.25}[\text{NTf}_2]_{0.75}$ with increasing AAP concentration. The horizontal line represents the resonance in pure $[\text{EMIM}][\text{NTf}_2]$.

The intermolecular interactions were more closely studied using NMR and IR spectroscopy. In the NMR investigations, the chemical shifts of the IL and AAP ^1H and ^{13}C signals were monitored in neat $[\text{EMIM}][\text{OAc}]_{0.25}[\text{NTf}_2]_{0.75}$ with varying amounts of AAP included. An internal acetone- d_6 capillary was used as a lock and chemical shift reference. The most informative NMR signal is the 2-H of the $[\text{EMIM}]$ cation as this provides the most direct information regarding hydrogen bonding and Coulombic interactions of the IL. Fig. 2 depicts these resonances, normalized to pure $[\text{EMIM}][\text{OAc}]_{0.25}[\text{NTf}_2]_{0.75}$, with the other NMR resonances summarized and discussed in the ESI (Tables S1 and S2) as are the IR spectra (Fig. S4).

The addition of AAP leads to a monotonic upfield shift of the $[\text{EMIM}]^+$ 2-H resonance (Fig. 2). This shift is consistent with

reduced hydrogen bonding and Coulombic interactions between $[\text{EMIM}]^+$ and $[\text{OAc}]^-$.¹⁸ Notably, at 2:1 AAP: $[\text{OAc}]^-$, the $[\text{EMIM}]^+$ 2-H chemical shift is approximately equivalent to neat $[\text{EMIM}][\text{NTf}_2]$ implying that AAP is effectively shielding $[\text{OAc}]^-$ anions from the $[\text{EMIM}]^+$ cation due to hydrogen bonding interactions and steric bulk. This is consistent with this ratio being the saturation concentration of AAP as it appears there are no free $[\text{OAc}]^-$ anions available for further hydrogen bonding interactions. IR analysis (Fig. S4) indicates that the hydrogen bonds with the $[\text{OAc}]^-$ anion arise primarily from the phenolic OH group with a secondary contribution from the amide functionality. The other NMR resonances (ESI) reiterate the secondary effect of the amide group and further demonstrate that hydrogen bonding appears to exclusively affect the $[\text{OAc}]^-$ anion with no detectable effect on the $[\text{NTf}_2]^-$ anion.

To investigate the propensity of strongly hydrogen bond donating cosolvents to compete with hydrogen bonding interactions between AAP and the IL $[\text{OAc}]^-$ anion, three solvents with varying hydrogen bond donor strength were investigated; ethanol (EtOH), acetic acid (AcOH) and 1,1,1,3,3,3-hexafluoroisopropanol (HFIPA). The hydrogen bond acidity of these solvents increases in the order EtOH < AcOH < HFIPA and Brønsted acidity increases EtOH < HFIPA < AcOH. The effect of these cosolvents on AAP solubility within $[\text{EMIM}][\text{OAc}]_{0.25}[\text{NTf}_2]_{0.75}$ was investigated (Fig. 3). Corresponding solubility curves for $[\text{EMIM}][\text{OAc}]_{0.50}[\text{NTf}_2]_{0.50}$ were obtained and are qualitatively similar (Fig. S9).

Three very different solubility profiles are observed for EtOH, AcOH and HFIPA (Fig. 3). EtOH exhibits approximately additive behavior with an almost linear relationship between solubility and EtOH mole fraction. AcOH demonstrates pronounced negative synergistic effects with a rapid decrease in solubility below additivity up to 0.50 mole fraction AcOH (4:1 AcOH: $[\text{OAc}]^-$) followed by a return towards additivity at higher AcOH concentrations. The most marked deviation is observed for HFIPA where a well-defined minimum occurs at 0.50 mole fraction HFIPA (4:1 HFIPA: $[\text{OAc}]^-$). This minimum represents a 89% and 93% decrease in solubility relative to pure HFIPA and pure $[\text{EMIM}][\text{OAc}]_{0.25}[\text{NTf}_2]_{0.75}$ respectively. Importantly, while negative synergistic effects have previously been reported in ILs,¹⁹ to the best of the authors' knowledge, such a large, well-defined solubility minimum has not been observed. The origin of this solubility behavior was investigated using a similar combination of NMR and IR spectroscopy as described for AAP (Figs. 4, S5–S7 and Tables S3–S8).

The magnitude of the chemical shift variation of the $[\text{EMIM}]^+$ 2-H signal increases in the order EtOH < AcOH < HFIPA (Fig. 4). Notably the chemical shift after 8 mole equivalents of HFIPA relative to the $[\text{OAc}]^-$ anion is the same as in pure $[\text{EMIM}][\text{NTf}_2]$. The magnitude of the OH resonance upfield shift of each antisolvent

accords with the order observed for the 2-H proton (ESI), reinforcing the likelihood that the 2-H chemical shift variation is due to hydrogen bonding. The other NMR signals (ESI) suggest that, as

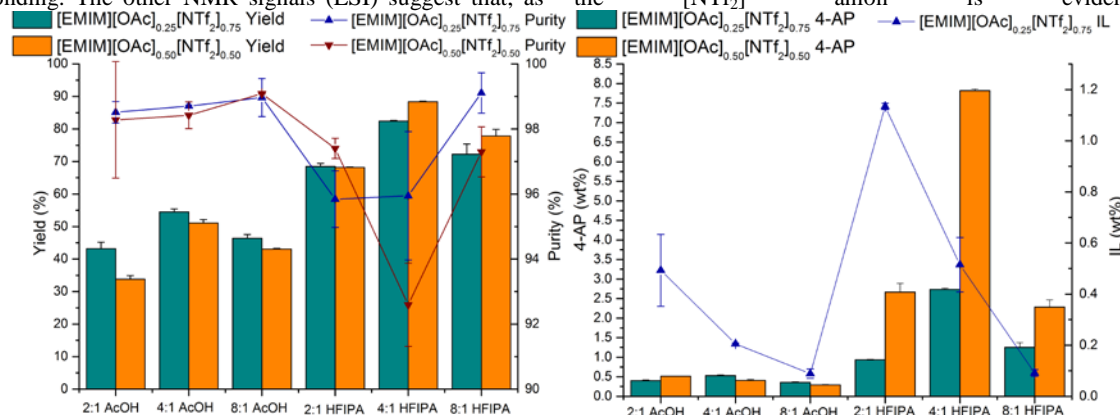


Fig. 5 Crystallization results for AAP crystallized from [EMIM][OAc]_x[NTf₂]_{1-x} using different antisolvent:[OAc]⁻ ratios. (Left) Yield and purity, determined by HPLC; (Right) 4-AP inclusion determined by HPLC and IL quantified by LC-MS. LC-MS analysis was not conducted on [EMIM][OAc]_{0.50}[NTf₂]_{0.50} samples but NMR analysis indicated similar trends were observed (Table S11). Reported errors are standard deviations from at least 2 replicate experiments.

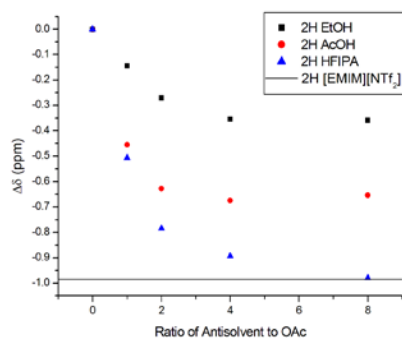


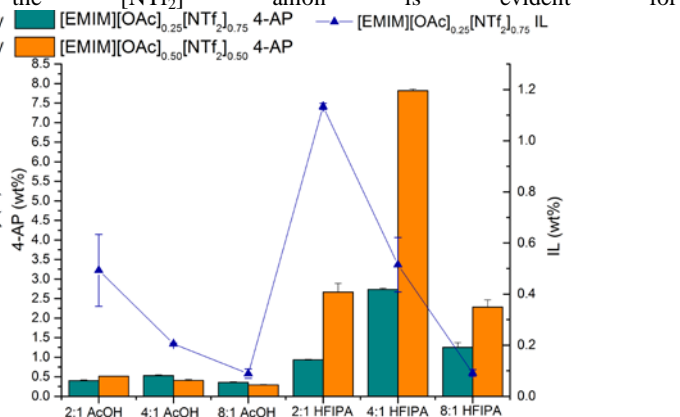
Fig. 4 ¹H NMR chemical shift of [EMIM]⁺ 2-H resonance in neat [EMIM][OAc]_{0.25}[NTf₂]_{0.75} with increasing EtOH, AcOH and HFIPA concentration.

AcOH and EtOH. The interactions with HFIPA lead to an upfield rather than the expected downfield shift of the CF₃¹³C resonance for the [NTf₂]⁻ anion, suggesting that fluorine interactions may dominate over hydrogen bonding in this case. These interactions are not observed until after the 2:1 stoichiometry and therefore would not be involved in the significant reduction in AAP solubility.

The IR spectra (ESI) are broadly in agreement with the results of the NMR investigation and depict antisolvent–IL interactions increasing in the order of hydrogen bond donating strength. Collectively the solubility data, NMR and IR spectra suggest that AcOH and HFIPA form strong hydrogen bonding complexes with the [OAc]⁻ anion. These complexes possess a stoichiometry between 2:1 and 4:1 unlike AAP which forms 2:1 complexes. The formation of oligomeric anions from strong hydrogen bonding interactions has been reported between AcOH and [OAc]⁻ and similar species could account for the results obtained for HFIPA, AcOH and AAP.²⁰ The increased stoichiometry of the cosolvent complexes may arise from their reduced steric bulk which allows more cosolvent molecules to interact with the [OAc]⁻ anion without resulting in steric clashes.

Given the ability to tune the solubility of AAP using these hydrogen bonding interactions, it was of interest to probe their effect on its crystallization. To examine the influence of these antisolvents on purification, 10 wt% 4-AP in AAP was used as a model impurity system and different concentrations of AcOH and HFIPA (2:1, 4:1 or 8:1 relative to [OAc]⁻) were used. EtOH was not used as the solubility measurements indicated that it would not lead to AAP crystallization. [OAc]⁻ concentration in the solvent was also varied

expected, hydrogen bonding interactions occur preferentially with the [OAc]⁻ rather than [NTf₂]⁻ in all cases. Hydrogen bonding with the [NTf₂]⁻ anion is evident for



with the ILs [EMIM][OAc]_{0.25}[NTf₂]_{0.75} and [EMIM][OAc]_{0.50}[NTf₂]_{0.50} both used as solvents. Crystallizations were conducted by the rapid addition of the antisolvent to the stirred homogenous IL solution at 25 °C with the resultant slurry stirred for 1 h before being filtered, washed with dichloromethane (2 × 5 mL) and dried at the pump. Yield, purity and 4-AP inclusion for each sample was determined by HPLC and the IL inclusion for [EMIM][OAc]_{0.25}[NTf₂]_{0.75} samples measured by LC-MS. The results are depicted in Fig. 5. The rate of antisolvent addition did not appear to influence the final purification results as slow addition of antisolvent over 1 h led to similar outcomes (Table S9). There was also no evidence of the formation of different polymorphs with XRD analysis of all crystallized AAP indicating the presence of form 1, the most stable form (Fig. S10).

Two predominant trends are evident from Fig. 5. The first is that IL inclusion generally decreases with increasing antisolvent concentration. This implies that IL inclusion is dominated by mass transfer where increased antisolvent concentration reduces the viscosity of the solution making the AAP crystals more amenable to efficient washing. Interestingly, the composition of the included IL differs from the initial [EMIM][OAc]_{0.25}[NTf₂]_{0.75} solution with a substantially higher proportion of [EMIM][OAc] retained, indicating that [EMIM][NTf₂]⁻ is preferentially removed by washing with dichloromethane (Table S10). The second main trend in Fig. 5 is that when yields are maximized by using HFIPA as an antisolvent, 4-AP inclusion increases substantially. This is most pronounced at 4:1 HFIPA:[OAc]⁻ for [EMIM][OAc]_{0.50}[NTf₂]_{0.50} where 7.8 wt% 4-AP was observed, compared to 2.3 wt% for the 8:1 HFIPA:[OAc]⁻ despite a relatively modest increase in yield (88% compared to 78%). This phenomenon suggests that 4-AP co-precipitates with AAP. Given the 4-AP phenol group has a higher pK_a value than AAP (10.5 compared to 9.5 at 25 °C), it would be anticipated that it is a weaker hydrogen bond donor. 4-AP displacement by HFIPA would therefore be favored relative to AAP when both phenols are present in similar concentrations which would account for the substantial increase in 4-AP inclusion at higher yields. To examine this further, 4-nitrophenol (4-NP) and 4'-chloroacetanilide (4'-CA) were used as model impurities for AAP in crystallizations from [EMIM][OAc]_{0.50}[NTf₂]_{0.50} using 4:1 and 8:1 antisolvent:[OAc]⁻ concentrations for AcOH and HFIPA. 4-NP has a lower pK_a than AAP and therefore should be a stronger hydrogen bond donor and 4'-CA does not contain the phenol moiety and hence hydrogen

bonding interactions should be less significant. The results of these experiments are compared with the results for 4-AP in Fig. 6.

Fig. 6 clearly shows the exponential increase in 4-AP inclusion with increasing crystallization yield. Neither 4'-CA nor 4-NP demonstrate the same increase as both exhibit a relatively linear increase in inclusion with yield. The relative order of inclusion suggests that hydrogen bonding with the IL anion may be a determining factor for impurity incorporation in AAP. That is, the low extent of 4-NP incorporation may be due to its stronger interactions with the solvent leading to a more favorable free energy of solvation and reduced tendency for inclusion into the AAP crystal lattice. Crystallization of AAP from conventional organic solvents using similar conditions gave the same order of inclusion (Tables S12 and S13), i.e. 4-NP < 4'-CA < 4-AP which appears to indicate this order is innate and not due to the strong solvent interactions. However, the organic solvent results were obtained at lower yields (<50%) so care must be taken in extrapolating these results to higher yields.

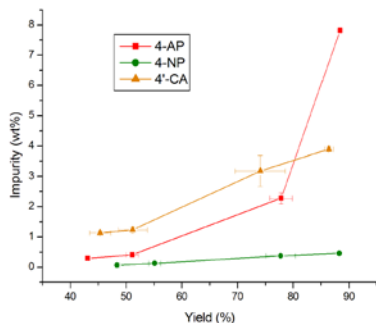


Fig 6. Comparison of impurity inclusion against yield for different model impurities in the crystallization of AAP from the IL [EMIM][OAc]_{0.50}[NTf₂]_{0.50} using AcOH and HFIPA as antisolvents. Lines are drawn between points as a guide for the eye, reported errors are standard deviations from at least 2 replicate experiments.

In summary, the interplay between hydrogen bonding interactions has been manipulated to tailor the solubility of AAP within ILs and engineer its crystallization through the use of strong hydrogen bond donating 'antisolvents'. The manipulation of such interactions led to isothermal crystallization yields of greater than 88% at 25 °C. The extent of purification of the crystallization process was in part dependent on the hydrogen bond strength of the impurity, with coprecipitation of the more weakly hydrogen bond donating 4-AP with no such behavior observed for 4-NP nor 4'-CA. This approach indicates the importance of understanding the interplay between molecular interactions for crystallization processes and demonstrates that by appropriately engineering these interactions, a wider variety of antisolvent combinations and the potential for increased crystallization yields are possible.

The authors thank Dr Gary Byrd and Dr Sunia Trauger from the Harvard Small Molecule Mass Spectrometry Facility for their assistance with LC-MS measurements. Support for this project from Novartis is gratefully acknowledged.

Notes and references

^a Novartis-MIT Center for Continuous Manufacturing and Department of Chemical Engineering, Massachusetts Institute of Technology, Cambridge, Massachusetts, USA

^b Center for Green Manufacturing and Department of Chemistry, The University of Alabama, Tuscaloosa, Alabama, USA

Electronic Supplementary Information (ESI) available: Experimental details, IR, NMR and XRD data, further crystallization data, analysis and discussion. See DOI: 10.1039/c000000x/

- M. Giuliatti and A. Bernardo, in *Crystallization - Science and Technology*, ed. M. R. B. Andreetta, InTech, 2012, pp. 379-396.
- (a) P. A. Meenan, S. R. Anderson and D. L. Klug, in *Handbook of Industrial Crystallization*, ed. A. S. Myerson, Butterworth-Heinemann, Boston, USA, 2002, pp. 67-100; (b) M. Lahav and L. Leiserowitz, *Cryst. Growth Des.*, 2006, **6**, 619; (c) M. Kitamura, *CrystEngComm*, 2009, **11**, 949.
- (a) P. Wasserscheid and W. Keim, *Angew. Chem. Int. Ed.*, 2000, **39**, 3772; (b) H. Weingartner, *Angew. Chem. Int. Ed.*, 2008, **47**, 654.
- J. P. Hallett and T. Welton, *Chem. Rev.*, 2011, **111**, 3508.
- (a) D. M. Fox, W. H. Awad, J. W. Gilman, P. H. Maupin, H. C. De Long and P. C. Trulove, *Green Chem.*, 2003, **5**, 724; (b) D. M. Fox, J. W. Gilman, A. B. Morgan, J. R. Shields, P. H. Maupin, R. E. Lyon, H. C. De Long and P. C. Trulove, *Ind. Eng. Chem. Res.*, 2008, **47**, 6327.
- V. N. Emel'yanenko, S. P. Verevkin and A. Heintz, *J. Am. Chem. Soc.*, 2007, **129**, 3930.
- (a) H. Niedermeyer, J. P. Hallett, I. J. Villar-Garcia, P. A. Hunt and T. Welton, *Chem. Soc. Rev.*, 2012, **41**, 7780; (b) G. Chatel, J. F. B. Pereira, V. Debbeti, H. Wang and R. D. Rogers, *Green Chem.*, 2014, **16**, 2051.
- (a) H. Mizuuchi, V. Jaitely, S. Murdan and A. T. Florence, *Eur. J. Pharm. Sci.*, 2008, **33**, 326; (b) K. B. Smith, R. H. Bridson and G. A. Leeke, *J. Chem. Eng. Data*, 2011, **56**, 2039; (c) J. R. de Azevedo, J.-J. Letourneau, F. Espitalier and M. I. Re, *J. Chem. Eng. Data*, 2014, **59**, 1766.
- H. Wang, G. Gurau, S. P. Kelley, A. S. Myerson and R. D. Rogers, *RSC Adv.*, 2013, **3**, 10019.
- (a) K. Bica and R. D. Rogers, *Chem. Commun.*, 2010, **46**, 1215; (b) P. M. Dean, J. Turanjanin, M. Yoshizawa-Fujita, D. R. MacFarlane and J. L. Scott, *Cryst. Growth Des.*, 2009, **9**, 1137; (c) W. L. Hough, M. Smiglak, H. Rodriguez, R. P. Swatloski, S. K. Spear, D. T. Daly, J. Pernak, J. E. Grisel, R. D. Carliss, M. D. Soutullo, J. H. Davis, Jr. and R. D. Rogers, *New J. Chem.*, 2007, **31**, 1429; (d) O. A. Cojocar, K. Bica, G. Gurau, A. Narita, P. D. McCrary, J. L. Shamshina, P. S. Barber and R. D. Rogers, *Nat. Chem. Commun.*, 2013, **4**, 559.
- (a) M. Kowacz, P. Groves, J. M. S. S. Esperanca and L. P. N. Rebelo, *Cryst. Growth Des.*, 2011, **11**, 684; (b) W. M. Reichert, J. D. Holbrey, K. B. Vigour, T. D. Morgan, G. A. Broker and R. D. Rogers, *Chem. Commun.*, 2006, 4767; (c) C. C. Weber, A. F. Masters and T. Maschmeyer, *Green Chem.*, 2013, **15**, 2655.
- (a) K. B. Smith, R. H. Bridson and G. A. Leeke, *CrystEngComm*, 2014, **16**, 10797; (b) J.-H. An and W.-S. Kim, *Cryst. Growth Des.*, 2013, **13**, 31; (c) J.-H. An, J.-M. Kim, S.-M. Chang and W.-S. Kim, *Cryst. Growth Des.*, 2010, **10**, 3044.
- M. Moniruzzaman and M. Goto, *J. Chem. Eng. Jpn.*, 2011, **44**, 370.
- M. A. Ab Rani, A. Brant, L. Crowhurst, A. Dolan, M. Y. Lui, N. H. Hassan, J. P. Hallett, P. A. Hunt, H. Niedermeyer, J. M. Perez-Arlandis, M. Schrems, T. Welton and R. Wilding, *Phys. Chem. Chem. Phys.*, 2011, **13**, 16831.
- (a) J. D. Holbrey, W. M. Reichert, M. Nieuwenhuyzen, O. Sheppard, C. Hardacre and R. D. Rogers, *Chem. Commun.*, 2003, 1636; (b) J. F. B. Pereira, L. A. Flores, H. Wang and R. D. Rogers, *Chem. Eur. J.*, 2014, **20**, 15482.
- L. Crowhurst, P. R. Mawdsley, J. M. Perez-Arlandis, P. A. Salter and T. Welton, *Phys. Chem. Chem. Phys.*, 2003, **5**, 2790.
- (a) K. Bica, J. Shamshina, W. L. Hough, D. R. MacFarlane and R. D. Rogers, *Chem. Commun.*, 2011, **47**, 2267; (b) H. Wang, G. Gurau, J. Shamshina, O. A. Cojocar, J. Janikowski, D. R. MacFarlane, J. H. Davis, Jr. and R. D. Rogers, *Chem. Sci.*, 2014, **5**, 3449.
- (a) R. Lungwitz and S. Spange, *New J. Chem.*, 2008, **32**, 392; (b) R. Lungwitz, M. Friedrich, W. Linert and S. Spange, *New J. Chem.*, 2008, **32**, 1493.
- E. Panteli and E. Voutsas, *Fluid Phase Equilib.*, 2010, **295**, 208.
- K. M. Johansson, E. I. Izgorodina, M. Forsyth, D. R. MacFarlane and K. R. Seddon, *Phys. Chem. Chem. Phys.*, 2008, **10**, 2972.